An immunomodulatory miniaturized screening 3D platform using liquefied capsules

COMPASS
ENGINEERING LIFE GUIDED BY NATURE

This paper must be cited as: Nadine, S., Correia, C. R., & Mano, J. F. An Immunomodulatory Miniaturized 3D Screening Platform Using Liquefied Capsules. *10*(10), 2001993. *Advanced Healthcare Materials*, (2021). https://doi.org/https://dx.doi.org/10.1002/adhm.202001993

An immunomodulatory miniaturized screening 3D platform using liquefied capsules

Sara Nadine, Clara R. Correia, João F. Mano**

S. Nadine, Dr. C. R. Correia, Prof. J. F. Mano

CICECO – Aveiro Institute of Materials, Department of Chemistry, University of Aveiro, Campus Universitário de Santiago, 3810-193 Aveiro, Portugal

Keywords: Immunomodulatory 3D Platform; Mesenchymal Stem Cells; Macrophages; Host's Immune Response; Polymers;

A critical determinant of successful clinical outcomes is the host's response to the biomaterial. Therefore, the prediction of the immunomodulatory bioperformance of biomedical devices following implantation is of utmost importance. Herein, we propose the use of liquefied capsules as immunomodulatory miniaturized 3D platforms for the high-content combinatorial screening of different polymers that could be used generically in scaffolds. Additionally, the confined and liquefied core of capsules affords a cell-mediated 3D assembly with bioinstructive microplatforms, allowing to study the potential synergistic effect that cells in tissue engineering therapies have on the immunological environment before implantation. As a proof-of-concept, three different polyelectrolytes, ranging in charge density and source, were used. Poly(L-lysine)-, alginate-, and chitosan-ending capsules with or without encapsulated mesenchymal stem/stromal cells (MSCs) are placed on top of a 2D culture of macrophages. Results show that chitosan-ending capsules, as well as the presence of MSCs, favors the balance of macrophage polarization towards a more regenerative profile, through the up-regulation of anti-inflammatory markers (CD163 and CCL13), and the release of pro-regenerative cytokines (IL-10 and VEGF). Overall, the developed system enables the study of the immunomodulatory bioperformance of several polymers in a cost-effective and scalable fashion, while the paracrine signaling between encapsulated cells and the immunological environment can be simultaneously evaluated.

1. Introduction

For a long time, most of the traditional tissue engineering devices were design to be biologically inert to avoid acute inflammatory responses. Nowadays, the paradigm has changed and there is ample evidence about how immune cells act positively during the regulation of tissue dynamics.[1] The repair process of most living tissues is followed by the activation of different types of innate immune cells, which strongly modulate tissue regeneration. In fact, the immune system plays a central role in determining the quality of the repair response, including the extent of wounding, and the precision to restore tissue and organ functions.[2] Among all immune cells, macrophages tend to be fundamental during all stages of the cascade events occurring during tissue repair. Derived from monocytes, macrophages become activated in response to signals present in damaged tissues or associated with pathogens. Macrophages are often referred to as having either an M1 or M2 profile, a simplified terminology based on their receptor expression, cytokines production, and function. The pro-inflammatory M1 macrophage phenotype is associated with pathogen killing and with classic signs of active inflammation. Otherwise, the anti-inflammatory M2 macrophage phenotype promotes immunoregulation, wound healing, and constructive tissue remodeling.[3] During tissue repair, only an efficient and precise timely switch from the pro-inflammatory M1 to pro-regenerative M2 macrophage phenotype results in an appropriate production of molecular cues crucial to support tissue healing response. Following a biomaterial implantation, dysregulation of the M2:M1 ratio leads to the formation of a collagenous fibrotic capsule surrounding and isolating the biomaterial, being the main cause for implant failure. Therefore, tissue engineering constructs able to direct and trigger an appropriate immunomodulatory repair responses towards tissue regeneration, while avoiding chronic inflammatory reaction, are of utmost importance.[4]

Usually, all biomaterials immediately initiate an immune response after implantation into a living tissue.[5] Ideally, every tissue engineering approach should be designed to target these immune early responders, while attracting key contributors, including progenitor or stem/stromal cells, and angiogenic factors, to leverage the regeneration process. Therefore, the

design of biomaterials should include factors known to influence their immunocompatibility, including the material's nature (natural or synthetic sources), molecular weight, charge density, or hydrophobicity/hydrophilicity.[6] The immunological responses are a crucial gateway for tissue repair and regeneration and the design of the biomaterial can dictate the success or failure of its integration. Besides the response of biomaterials alone, the combined effect of cells and biomaterials on the immune response is also relevant when considering the use of hybrid constructs for tissue engineering. Following this path, we consider that the development of immunomodulatory *in vitro* screening platforms able to provide a more predictive environment of the bioperformance of biomedical devices following implantation are of utmost importance. Deepening the understanding of the immunological profile of hybrid cell/biomaterial constructs is certainly a valuable opportunity to facilitate the translation of tissue engineering strategies into the clinics.

Herein, we propose an immunomodulatory miniaturized 3D platform using liquefied capsules for the *in vitro* combinatorial screening of multiple biomaterials and cells, as shown in **Scheme 1**. Such concept can help to identify candidate combinations of polymers and cells to be incorporated into a scaffold, while providing valuable information about their immunological profile. Moreover, the developed immunomodulatory 3D platform relies on the presence of a liquefied and confined core entirely suitable for the long-term encapsulation of cells and bioinstructive microplatforms, thereby simultaneously allowing to study the regenerative potential of the system. In particular, the permselective thin membrane enveloping the capsule will allow the paracrine communication of the inner cells with the external immune ecosystem, and consequently allowing to evaluate the biological outcome of such interaction.

The proposed immunomodulatory 3D platform is composed by: (i) a multilayered membrane wrapping the core contents, while ensuring permeability to essential molecules for cell survival; (ii) surface functionalized poly(ε-caprolactone) microparticles (μPCL) acting as cell adhesion domains for anchorage-dependent cells; and (iii) adipose-derived mesenchymal stem cells

(ASCs). Such liquefied capsules are then placed on top of a 2D culture of macrophages. The permselective membrane is developed through the layer-by-layer technology, which relies on the sequential deposition of nanolayers of oppositely charged polyelectrolytes. Simply by changing the last layer of the liquefied capsules, we envisioned to study the immunomodulatory effect of distinct polyelectrolyte while simultaneously modulating the behavior of externally cultured macrophages. Given the fact that polyelectrolytes can be divided into multiple classes considering the number of functional groups, pH and ionic strength, among other characteristics[7], we hypothesize that a multitude of immunological profiles can be established. For that, high-content systems enabling multi-parameter using small sample sizes and in a cost-effective and scalable fashion are desired. Furthermore, the proposed system also possesses a highly modular character. Either by changing the type of cells and microparticles encapsulated, or the type of functionalization employed to the nanolayered membrane, a plethora of different cell encapsulation systems can be formulated. Additionally, the bioinstructive microplatforms that supports the cells inside the capsule can present different topographical features and stiffness cues to govern cell orientation, migration, and/or differentiation *in vitro.* Recently, we demonstrated that nanogrooved microplatforms were able to induce the osteoblastic differentiation of stem cells even in the absence of osteoinductive factors.[8] Overall, the proposed immunomodulatory 3D platform is a high-content microsized device able to find the combination of polymers, cells, and bioinstructive cell adhesion sites that result in an enhanced regenerative potential using a simple but powerful high-content *in vitro* analysis. We intend to minimize the use of *in vivo* experiments by analyzing multiple polymers and understand their immunological response *in vitro*. Moreover, we expect that the small-scale capsules facilitate the evaluation of a broad number of biomaterials, providing incremental information considering the whole *in vivo* system in which a biomaterial is placed.

As a proof-of-concept, we used the developed immunomodulatory 3D platform to evaluate the influence of three polyelectrolytes from different sources and charges in human macrophages.

To build the layer-by-layer membrane, we used poly(L-lysine) (PLL), alginate (ALG), and chitosan (CHT) as polyelectrolytes. Then, we analyzed the potential synergistic effect that encapsulated ASCs have on the biological performance of macrophages. We believe that this platform will give important insights about the interaction of immune cells with stem cell encapsulation systems, and thus recreating in a more realistic fashion the native host versus graft response following tissue engineering devices implantation.

2. Results

2.1. Interaction between Liquefied Capsules and Macrophages

The successful development of Liquefied Capsules (LC) encapsulating poly(ε-caprolactone) microparticles (μPCL) was visualized by light microscopy (**Figure 1A**). After phorbol myristate acetate (PMA) treatment, THP-1 became adherent and the expression of the recognized macrophage marker CD36[9] was analyzed by immunofluorescence staining (**Figure 1B and Figure S1. A**) and by flow cytometry (**Figure S1. B**), to confirm the monocyte-to-macrophage differentiation. Then, liquefied capsules ending in PLL (synthetic positively charged polyelectrolyte), CHT (natural polyelectrolyte neutral at pH = 7.4), or ALG (natural negatively charged polyelectrolyte), were directly cultured on top of the 2D culture of THP-1 macrophages for 7 days. The CD36 surface expression continued constant in all conditions during 7 days of culture (**Figure S1. C**). Live-dead assay shows that, after 7 days of interaction with liquefied capsules, the majority of macrophages remained viable (**Figure 1C**). The viability of macrophages was above 80 % (**Figure S2. A**). The DNA quantification assay shows that the quantity of macrophages was maintained constant during the culture time (**Figure S4. A**). The fluorescence staining of F-actin filaments shows that liquefied capsules did not influence the macrophage morphology between the different last layers (**Figure 1D**). However,

comparing with the control, macrophages looked more elongated and rather narrow shaped, suggesting their polarization into M2 macrophages. Although not statistically significant, a slight increase of the aspect ratio (measure of the stretching of a cell, i.e. [Major Axis]/[Minor Axis]) of cells was observed after co-culture with the liquefied capsules (**Figure S3**).

2.2. Influence of Liquefied Capsules over Macrophage Polarization

To evaluate the biocompatibility and immunomodulatory ability of each polymer, we observed the influence of each polyelectrolyte-ending layer of small-scale liquefied capsules over macrophage polarization. After interaction with cell-empty liquefied capsules, the metabolic activity of 2D macrophages was analyzed after 1, 4 and 7 days of culture. Results show that the interaction with liquefied capsules significantly enhanced the metabolic activity of macrophages up to 7 days of culture (**Figure 2B**). Comparing the different ending layers, PLL-ending liquefied capsules promoted the highest increase in the metabolic activity of macrophages. The cytokine profile of macrophages cultured in contact with cell-empty liquefied capsules was also analyzed. The release of the pro-inflammatory cytokine IL-6 increased for macrophages cultured with all liquefied capsules, particularly in the ALG- and CHT-ending liquefied capsules, after 7 days of culture (**Figure 2C**). On the other hand, at day 7, the secretion of the anti-inflammatory cytokine IL-10 was also overexpressed in all liquefied capsules (**Figure 2D**), and CHT-ending liquefied capsules presented the highest release. Notably, IL-6/IL-10 ratio significantly decreased over time, with a pronounced consistency for CHT (**Figure 2E**). Increased IL-6/IL-10 ratio is correlated with poor regeneration outcomes.[10,11] Remarkably, the gene expression of the pro-healing markers CCL13 and CD163 was up-regulated for PLL and CHT (**Figure 2H-I**), regardless a significant enhancement of inflammatory genes (CCL20/CXCL10) for PLL-ending liquefied capsules was observed (**Figure 2F-G**). Considering the profile expression of 2D macrophages interacting with

different cell-empty liquefied capsules, CHT-ending condition was chosen as the candidate that might maximize the pro-healing response of the developed system. Therefore, this condition was selected to encapsulate ASCs (LC-ASCs), and their possible synergistic effect with macrophages was further evaluated.

2.3. Impact of Encapsulated Cells over Macrophages

To further understand the paracrine signaling between encapsulated ASCs and macrophages, an indirect co-culture system was created. CHT-ending LC-ASCs were placed on top of a 2D culture of macrophages (**Figure 3A**). Live-dead assay shows that both phenotypic cells remained viable up to 7 days of culture. The viability of macrophages and ASCs was above 90 % (**Figure S2. B**). The DNA content of ASCs significantly increased during the 7 days of culture, indicating the ability of liquefied capsules to support cell proliferation (**Figure S4. B**). Additionally, macrophages and ASCs showed an increasing metabolic activity over time (**Figure 3B**). The profile of vascular endothelial growth factor (VEGF), IL-6 and IL-10 released by macrophages and ASCs was also evaluated. Of note, the release of cytokines was measured in the culture medium, thus in the external environment of liquefied capsules, which is enabled by the permeability of the multilayered membrane to biomolecules, as we previously observed for bone morphogenic protein (BMP)-2 and VEGF.[12] A plain-culture of encapsulated ASCs and chitosan-ending capsules (Mϕ+LC) were used as control. Interestingly, the paracrine signaling between macrophages and ASCs led to an enhanced release of VEGF (**Figure 3C**). VEGF is a vascular growth factor involved in the development of new blood vessels and, therefore, critical for tissue regeneration.[13] Likewise, the pro-inflammatory cytokine IL-6 was also significantly higher when macrophages were co-cultured with LC-ASCs (**Figure 3D**). However, this was only observed at day 1. With increasing culture times, the release of IL-6 by ASCs reaches similar levels of those observed in the co-culture of macrophages with LC-ASCs.

On the other hand, the secretion of the anti-inflammatory cytokine IL-10 significantly increased when macrophages were co-cultured with LC-ASCs (**Figure 3E**). The release of IL-10 by the plain-culture of encapsulated ASCs was almost null. Furthermore, the IL-6/IL-10 ratio significantly decreased after 4 and 7 days of culture for the indirect co-culture, while it significantly increased for the plain-culture of encapsulated ASCs (**Figure 3F**).

The quantification of the transcripts for the pro-inflammatory CXCL10 and CCL20, and the pro-healing CCL13 and CD163 genes was performed at 1, 4, and 7 days of culture. The gene expression of pro-inflammatory CXCL10 and CCL20 markers decreased with increased culture periods, with a significant difference for CCL20 (**Figure 4A-B**). An opposite trend was found for the expression of the pro-healing CCL13 and CD163 markers, although a slight downregulation is observed at day 7 for the CD163 marker (**Figure 4C-D**). Moreover, analyzing the seventh day of culture, the expression of the CD163 anti-inflammatory marker was significantly increased with the presence of ASCs (**Figure 4D**). Additionally, the expression profile of surface markers of macrophages was assessed after 7 days of culture. The phenotypical profile of macrophages cultured in 2D (Mϕ), macrophages cultured with CHT-ending liquefied capsules (Mϕ+LC), and macrophages indirectly cultured with encapsulated ASCs (Mϕ+LC-ASCs), was characterized by the expression of CD80 and CD163 by flow cytometry (**Figure 4E**). No differences were observed for the expression of the M2-like marker CD163 comparing the 2D culture of macrophages (7.26 %) and macrophages interacting with CHT-ending liquefied capsules (8.83 %). However, the indirect co-culture between macrophages and ASCs led to a remarkably enhancement of the expression of the pro-healing CD163 marker (41.2 %), along with a small expression of the pro-inflammatory CD80 marker (8.97 %).

3. Discussion

Until very recently, the immune system's response to biomaterials was viewed as detrimental and with negative implications in tissue healing outcomes. Nowadays, it is well established that immune cells can play both positive and negative roles in the pathogenesis of diseases and tissue remodeling.[14,15] Among all innate immune cells, macrophages have received the most attention as a significant modulator of diseases and tissue repair following injury.[16] Macrophages are monocyte-derived myeloid cells that differentiate upon emigration from the blood vessels into the tissue. Depending on the tissue type, microenvironmental conditions, and the immunologic milieu, macrophages may undergo differentiation into a number of distinct phenotypes.[17] Mimicking the Th1/Th2 nomenclature which has been described for T helper cells, polarized macrophages are defined as having either an M1 or an M2 phenotype, depending on their functional properties and patterns of gene expression.[18] Polarization into classically activated M1 macrophages results from the interaction with pro-inflammatory signals such as interferon-γ (IFN-γ) and endotoxins such as lipopolysaccharide (LPS), while alternatively activated M2 macrophages are induced by a variety of anti-inflammatory signals including IL-4, IL-13, and IL-10, as well as, immune complexes, and glucocorticoids.[19] These innate immune cells are fundamental to maintain tissue homeostasis by mediating multiple cellular events, namely proliferation, angiogenesis, and the deposition of extracellular matrix (ECM). Either by trauma or simply by the implantation of a biomaterial, it is fundamental to have an efficient and timely macrophage's phenotypic switch for a proper and functional tissue remodeling. If the host immune system fails to increase M2 macrophage levels, it could lead to the inability to resolve excessive inflammation.[4] On the other hand, prolonged presence of M2 macrophages can lead to the formation of detrimental foreign body giant cells (FBGCs).[15] Therefore, the design of immunomodulatory smart biomaterials to control this M2:M1 ratio is crucial to ameliorate the outcomes of medical implants and tissue engineering therapies. Previously, we have studied in 2D the influence of different surface modifications performed on poly(L-lactic acid) films on the differentiation of human monocytes into macrophages.[20]

Indeed, the success of a biomaterial implantation is largely correlated with their microenvironmental cues that can control inflammatory responses towards healing and regeneration. Therefore, the deficit in understanding the interaction of macrophages with the biomaterials *in vitro,* and the unpredictable nature of how such kind of interactions could occur[21], led us to envision a 3D immunomodulatory platform for the high-throughput combinatorial screening of different biomaterials and cells. The proposed concept relies on the production of alginate-based microgels encapsulating cells and microparticles by ionotropic gelation, followed by coating with permselective polymeric layers, and core liquefaction. Here, the multilayered membrane wraps all the cargo content and ensures the high diffusion of essential molecules for cell survival. Furthermore, microparticles can act as cell adhesion sites, allowing cells to adhere and proliferate, and eventually differentiate when stem cells are used. The liquefied capsules were already tested as a cell encapsulation system for tissue engineering applications in an alternative to avoid the use of conventional scaffolds with fixed geometries and open surgery implantations, while also be injectable by minimally invasive procedures.[12,22–26] The system was already tested *in vivo*, however, due to the use of immunocompromised mice models, the interaction with the immune system remains uncertain.[24] Herein, we envisioned the use of liquefied capsules as an immunomodulatory *in vitro* screening platform able to provide a more predictive environment of the bioperformance of biomedical devices following implantation. Besides the response of biomaterials alone, the combined effect of cells and biomaterials on the immune response is also relevant in hybrid constructs for tissue engineering. Following this path, we consider that deepening the understanding of the immunological profile of hybrid cell/biomaterial constructs is certainly a valuable opportunity to facilitate the translation of tissue engineering strategies into the clinics. The fabrication of the multilayered membrane is based on electrostatic interactions of oppositely charged polyelectrolytes.[27] To demonstrate the potential of the platform to test a long variety of biomaterials, three different polyelectrolytes with quite distinct chemical natures

were used, namely a synthetic positive charged polyelectrolyte (poly(L-lysine) (PLL)), a natural negative charged polyelectrolyte (alginate (ALG)), and a natural polyelectrolyte neutral at pH ~ 7 (chitosan (CHT)). The obtained 12-layered membrane (around 110 nm) is "permselective" to relevant bioproducts (e.g. nutrients, oxygen, metabolites, waste products, cell signalling), and avoids the entrance of larger components (e.g. immunoglobulins, and immune cells). Initially, the influence of different types of polyelectrolytes in the last layer of the capsules when in contact with macrophages was evaluated. For that, cell-empty liquefied capsules were directly cultured on top of a 2D culture of macrophages. Independently of the polyelectrolyte present in the last layer of liquefied capsules, the cellular viability of macrophages remained uncompromised (Figure 1C). Nevertheless, macrophages in contact with the different formulations of liquefied capsules became more elongated and rather narrow shaped, comparing with the control (Figure 1D). Morphological alterations *in vitro* were already reported followed macrophage polarization. While M1 macrophages presented flattened and round shape, the polarization into M2 macrophages induce an elongated cell shape.[28] Additionally, the presence of liquefied capsules led to an enhancement in the metabolic activity of macrophages. All the polyelectrolytes tested, namely PLL, ALG, and CHT, induced an enhanced reduction of the tetrazolium compound into formazan via glycolytic NADH production, compared with the control (**Figure 2B**). However, significant variations between the three polyelectrolytes were noticed after cytokine profile and genotypic analysis. Macrophages can release a wide range of inflammatory mediators in response to external signals. Moreover, tissue regeneration is intimately linked with a proper sequence of inflammatory molecules followed by anti-inflammatory signals.[3,29,30] Therefore, after determining the cytokine profile of macrophages cultured in contact with the liquefied capsules ending with different polyelectrolytes, it was possible to confirm a significant increase of the release of the pro-inflammatory cytokine IL-6 (**Figure 2C**). In fact, the administration of pro-inflammatory cytokines to fracture sites immediately after injury accelerated fracture repair in

mice.[31] However, sustained administration as well as prolonged inflammation is associated with impaired healing.[31,32] Therefore, if they subside in a timely fashion, pro-inflammatory cytokines are essential for tissue repair. The release of the anti-inflammatory cytokine IL-10 also increased over time for all liquefied capsules (**Figure 2D**). IL-10 is one of the most studied anti-inflammatory cytokines, and it is crucial in restraining inflammation.[33] Associated to M2 macrophages, IL-10 is not only necessary for the M1-M2 phenotype switch, but also indispensable for scar-free healing of wound and heart tissues.[34,35] Remarkably, IL-6/IL-10 ratio significantly decreased over time, with a significant consistency for CHT (**Figure 2E**). IL-6/IL-10 ratio is a valuable prognosticator of the pro- versus anti-inflammatory balance.[10,11] Given the importance of the M1 to M2 macrophage polarization during tissue regeneration, we observed the gene expression of macrophages when interacting with the small-scale capsules (**Figure 2F-I**). Results show that after 7 days of culture, ALG behaved as an inert material since it did not induce the expression of both pro- and anti-inflammatory markers. ALG is a natural-derived anionic polysaccharide widely used in cell encapsulation technologies. Although induction of foreign body reaction and fibrosis have been reported, alginate usually do not elicit an immune response.[36–38] Some studies suggested that the G:M ratio can be directly related with alginate's biocompatibility, and its effect on macrophage polarization.[39] The geometry and the size of the implanted material also influence the recognition of alginate by the host. The spherical geometry and size above 1.5 mm in diameter were shown to significantly improve biocompatibility when compared with smaller-sized or differently shaped counterparts.[40] On the contrary, PLL and CHT induced the expression of pro-healing CCL13 and CD163 markers (**Figure 2H-I**). However, pro-inflammatory markers (CXCL10 and CLL20) were likewise significantly expressed for PLL-ending capsules (**Figure 2F-G**).[41] PLL is a synthetic polymer commonly used to improve cell adhesion and proliferation.[42] Despite the fact that PLL is known to be immunogenic and evokes inflammatory responses, recent results show that PLL influence macrophages towards the M2 polarization.[43–45] On the other hand, CHT is a

biodegradable polysaccharide derived from chitin which possesses an inherent antimicrobial activity.[46] Its immunomodulatory properties are poorly understood, however some studies have shown that CHT is a powerful activator of macrophage's inflammasomes, while others demonstrated CHT's modulatory capacity to polarize macrophages into a M2 anti-inflammatory phenotype.[46–50] Indeed, the inflammatory response depends on prior immune cell activation state, CHT dose, and degree of acetylation.[51] After analysis of cytokine profile and gene expression, CHT-ending liquefied capsules have been shown to favor the immunomodulatory response compared to ALG and PLL, since an up-regulation of pro-healing molecules and down-regulation of pro-inflammatory markers was observed. Since the liquefied capsules are in direct contact with macrophages, resembling the microenvironment of the implantation process, the obtained outcomes from the last layer of the 3D immunomodulatory platform may be translated to others commonly used implant systems using the same polymer. The next step was to evaluate the synergistic effect of liquefied capsules encapsulating ASCs with macrophage polarization. This is a necessary validation if we intend to use the platform to screen hybrid constructs for tissue engineering applications. For that, liquefied capsules were used to develop an indirect co-culture system relying on CHT-ending liquefied capsules encapsulating ASCs and placed on top of a 2D culture of macrophages. ASCs are very interesting mesenchymal stem cells due to their multilineage differentiation potential, relatively simple process of accessing and isolating, and being available in large quantities with minimal donor site morbidity.[52] After 7 days of encapsulation, ASCs remained viable and their metabolic activity significantly increased over time (**Figure 3A-B**). Furthermore, the co-culture system allowed to release the highest amount of VEGF (**Figure 3C**), evidencing that the paracrine signaling between ASCs and macrophages may prompt blood vessels formation through the recruitment of endothelial cells. In fact, it is well-known that both ASCs and macrophages are involved in secreting the pro-angiogenic factor VEGF.[53–56] Previously, we have detected in the culture medium the presence of cytokines such as BMP-2 and VEGF

released by encapsulated cells, indicating that these molecular factors are able to cross the nanolayered membrane of the liquefied capsules.[12] The semi-permeability inherent to the multilayered membrane is of utmost importance, since after implantation the encapsulated cells can interact with the surrounding environment by signaling molecules. Thus, the encapsulated mesenchymal stem cells may recruit macrophages into the wound, and promote wound healing.[57] Additionally, the combined effect of ASCs and macrophages led to a significant increase of the anti-inflammatory cytokine IL-10 content and a decrease in the IL-6/IL-10 ratio profile (**Figure 3E-F**). Although the release of IL-6 was constant, such results indicate that there is a polarization of the microenvironment into a regenerative profile (**Figure 3D**). Similarly to the results observed in cell-empty liquefied capsules (Mϕ+LC), the presence of ASCs significantly enhanced the release of the anti-inflammatory cytokine IL-10. The immunomodulatory properties of stem cells over macrophages were already observed in 3D cultures, triggering a less inflammatory macrophage profile by down-regulating inflammatory molecules and up-regulating regenerative markers, which is favorable for wound resolution.[58,59] The immunomodulatory ability of stem cells were also established *in vivo*, where a partially attenuated foreign body reaction following hydrogel implantation was observed.[60] Thus, it is expectable that after implantation of a chitosan-ending construct encapsulating ASCs, the recruited macrophages will be stimulated towards a down-regulation of pro-inflammatory markers (CXCL10 and CCL20) and an up-regulation of pro-regenerative markers (CCL13 and CD163), as shown after gene expression quantification with the liquefied capsules (**Figure 4A-D**). To reinforce such results, after 7 days of co-culture, macrophages showed an enhancement in the cell surface marker CD163, commonly present in M2 macrophages, while CD80 was maintained relatively low (**Figure 4E**).

Nowadays, insights on how biomaterials can mitigate the foreign-body reaction and improve engraftment are of utmost importance. In addition, it is necessary to have a better understanding of the entire immune system during tissue regeneration to establish a set of design principles to

aid in the engineering of a new generation of immuno-informed biomaterials. Here, we demonstrated the potential of liquefied capsules to differentially regulate macrophage behavior simply by changing the last layer of the system. One of the main benefits of the platform is their cost-effectiveness and scalability. From the same batch of liquefied capsules encapsulating cells and bioinstructive microparticles, several polymers can be evaluated simply by performing another polyelectrolyte deposition. Of note, the platform allows the decoupled analysis of the two parameters, namely the polyelectrolyte effect or the presence of encapsulated cells, since in all the multiple formulations of polyelectrolyte-ending capsules the encapsulated cells are always in direct contact with the same polyelectrolyte, namely poly(L-lysine). The proposed immunomodulatory 3D platform is also versatile. This system can be set up without the use of microparticles, to mimic strategies based on suspended/non-aggregated cell-in-gel systems using suspensions of cells instead of aggregates of cells and microparticles. The viscosity of the liquefied core can be also modified, allowing to resemble other types of strategies when the purpose is to evaluate the effect of cells on the phenotype of macrophage.

Herein, chitosan was the polyelectrolyte that disrupted the balance of macrophage polarization towards a favorable anti-inflammatory and regenerative profile. The study also highlighted the immunomodulatory ability by ASCs on the polarization of macrophage, while potentially harnessing the beneficial effects towards vascularization and tissue integration. Overall, this immunomodulatory process can be controlled either by changing the last layer of the liquefied capsules, or the cellular ecosystem composition inside the liquefied environment. The proposed platform is defined as a high content approach since it is possible to analyze multiple parameters at the same time. The immunomodulatory 3D platform allows to analyze different polymers simultaneously with the cellular ecosystem composition inside the liquefied environment. Bioinstructive microplatforms with different topographical features and stiffness cues can be added within the liquefied core, guiding cells to proliferate or differentiate towards a target lineage. Moreover, the complexity of the proposed miniaturized platform can be easily

increased to fulfil other requirements, such as the encapsulation of soluble factors that could then be released to the external environment through the permselective membrane,[12] the decoration of the last layer with bioinstructive signals (e.g. peptides or sugars),[21] or the effect of shear stress on the encapsulated cells, which can be easily achieved by using spinning flaks to create dynamic culture conditions due to the liquefied environment of the core.[25] We consider that this immunomodulatory miniaturized 3D platform will have a significant contribute to the tissue engineering field by performing the combinatorial screening of different polymers with different cells. Moreover, we believe that such platform will minimize the use of *in vivo* experiments, since to analyze the number of conditions proposed in this study, a large number of animals would be required.

4. Conclusion

Altogether, the present study showed the potential of using liquefied capsules as immunomodulatory 3D platforms for interrogating *in vitro* the decoupled influence of biomaterials and cells in the immune response. In tissue engineering strategies it is of utmost importance that an implanted biomaterial can be able to create a favorable microenvironment for tissue regeneration by controlling the host inflammatory response. Simply by changing the biomaterial of the last layer of the liquefied capsules, it is possible to proactively modulate the surrounding macrophages behavior, and at the same time, study independently the paracrine signaling with encapsulated cells. This *in vitro* microsized 3D platform allows the high-content combinatorial screening of polymers' candidates, while evaluating their influence on the response of immune cells. The imperativeness for more refined and clinically relevant model systems offers the ability to improve predictability, thus imposing the link between the *in vitro* studies and the *in vivo* clinical outcomes. Moreover, the encapsulation of immunomodulatory cells, such as ASCs, may change the activation states of macrophages and have important implications in the natural healing ability of a tissue. Given the highly modular character of the

developed platform, it can be easily adapted to fulfil the requirements for the bioengineering of multiple tissues or even be applied for other distinct purposes, ranging from bioengineered cell-containing constructs for basic biological research to *in vitro* platforms for disease modelling and drug screening.

5. Experimental Section

Cell culture: Adipose-derived mesenchymal stem cells (ASCs, passage 4, ATCC® PCS-500-011™) were cultured in α-MEM (minimum essential medium, ThermoFisher Scientific), supplemented with 10 % of heat-inactivated fetal bovine serum (FBS, ThermoFisher Scientific), 100 U mL^{-1} of penicillin and 0.1 mg mL^{-1} of streptomycin (ThermoFisher Scientific). For cell encapsulation purposes, ASCs were washed with PBS solution and detached using Tripsin-EDTA (Merck) for 5 min at 37 ºC. Every 3-4 days, fresh medium was added. Cells were counted and added to the alginate solution. Human monocytic cell line THP-1 (ATCC® TIB-202™) was cultured in RPMI 1640 medium with L-glutamine (ThermoFisher Scientific), supplemented with 10 % of heat-inactivated FBS, 100 U mL^{-1} of penicillin and 0.1 mg mL^{-1} of streptomycin, 10 mM HEPES (Merck), 1 % sodium pyruvate (ThermoFisher Scientific), and 1.2 g L^{-1} of sodium bicarbonate (Merck). Monocyte-derived macrophages (M0-like) were obtained after incubation with 50 ng ml^{-1} of phorbol myristate acetate (PMA, Merck) for 24 h, and additional 24 h in RPMI medium.

PCL microparticles production and functionalization: Surface functionalized poly(ε-caprolactone) microparticles (μPCL) were produced by emulsion solvent evaporation technique. Briefly, PCL (5 % w/v PCL, Mw ~ 80000, Merck) dissolved in methylene chloride (Honeywell) was slowly added to a stirring 0.5 % w/v polyvinyl alcohol (PVA, Merck) solution. Under agitation during 2 days at room temperature (RT), the produced μPCL were subsequently sieved to obtain a diameter range of 40-50 μm. The obtained μPCL presented a diameter of 45.62 ±

6.63 μm. Afterwards, surface modification was performed by placing μPCL into a low-pressure plasma reactor chamber (ATTO, Diener Electronic) fitted with a radio frequency generator. Air was used as gas atmosphere. A low-pressure glow discharge was generated at 30 V and 0.2-0.4 mbar for 15 min. Then, μPCL were immediately sterilized by UV-radiation for 30 min, and then immersed in an acetic acid solution (20 mM, Chem-Lab NV) containing collagen I (10 μg cm^{-2}, rat protein tail, ThermoFisher Scientific) for 4 hours at RT.

Liquefied Capsules production: ASCs were washed with PBS solution, detached using Tripsin-EDTA (Merck), and resuspended ($3x10^6$ cells per mL of alginate) in 2.0 % w/v of low viscosity sodium alginate from brown algae (9.5 cP, ALG, Merck), prepared in sodium chloride solution (0.15 M, LabChem) and containing 30 $mg{\cdot}mL^{-1}$ of μPCL. Then, microgels were obtained by the ionotropic gelation of ALG containing ASCs and μPCL in a calcium chloride (0.1 M, $CaCl_2$, Merck) solution. Subsequently, layer-by-layer is performed using poly(L-lysine) (PLL, Mw ~ 30 000–70 000, Merck), ALG, and chitosan (CHT, NovaMatrix) as polyelectrolytes (0.5 $mg{\cdot}mL^{-1}$), in order to produce the multilayered membrane. This process is repeated until a 12-layered membrane is created. Three different encapsulation systems were developed, each one ending with a different polyelectrolyte, namely PLL, ALG, and CHT. Ultimately, the liquefied core is obtained by chelation with ethylenediaminetetraacetic acid (5 mM, EDTA, Merck) for 5 min at RT. The pH of all solutions was set to 6.7, excepting for CHT (pH 6.3), and were sterilized by filtration using a 0.22 μm filter. After capsules production, THP-1 cells ($2.5x10^5$ cells per well) were cultured in 24 well-plates in RPMI 1640 supplemented medium and stimulated with PMA (50 ng per mL of RPMI 1640) for 24 h, and additional 24 h in RPMI medium, to obtain monocyte-derived macrophages. Then, capsules with or without ASCs and with variable last layers of polyelectrolytes (5 capsules per well) were added on top of 2D cultured macrophages. Samples were cultured up to 7 days at 37 ºC in a humidified 5 % CO_2 air atmosphere.

Live-dead assay: To assess the viability of macrophages and encapsulated ASCs, a live-dead fluorescence assay was performed according to the manufacturer's recommendation (ThermoFisher Scientific). Briefly, each sample was stained with calcein-AM (1:500 in PBS) and propidium iodide (1:1000 in PBS), for 15 min at 37 ºC, and protected from light. Afterwards, samples were immediately visualized by fluorescence microscopy (Axio Imager 2, Zeiss). ImageJ software was used to quantify cell viability based on the red color intensity of dead cells and green color intensity of viable cells.

Phalloidin/DAPI fluorescence staining: In order to observe cellular morphology, macrophages were stained for actin and nuclei. After 1, 4, and 7 days, samples were washed with PBS and fixed in formaldehyde (4% v/v) for 1 hour at RT. Then, samples were permeabilized with Triton X (0.1% (v/v), Merck) for 5 min, followed by incubation in Flash Phalloidin Red 594 (1:40 in PBS, Biolegend) for 45 min at RT. Cells nuclei were counterstained with DAPI (1:1000 in PBS, ThermoFisher Scientific) for 5 min. Following PBS washing, samples were visualized by fluorescence microscopy (Axio Imager 2, Zeiss). The aspect ratio of macrophages, defined by the [Major Axis]/[Minor Axis] ratio, was quantified using the ImageJ software.

Immunofluorescence labelling: After PMA stimulation, THP-1 cells cultured on coverslips were washed with PBS and fixed in formaldehyde (4% v/v) for 1 hour at RT. Then, cells were incubated with PE anti-human CD36 (5 µL of antibody per $1x10^6$ of cells, clone 5-271, Biolegend) to observe monocyte-to-macrophage differentiation. Undifferentiated monocytes were stained as control. Cells nuclei were counterstained with DAPI (1:1000 in PBS, ThermoFisher Scientific) for 5 min. Ultimately, labelled cells were visualized by fluorescence microscopy (Axio Imager 2, Zeiss).

DNA quantification: Total DNA quantification was performed for macrophages (in triplicate) and ASCs (n=5 per well in triplicate) separately, after cell lysis. Each sample of each well was

suspended in 500 µL of ultra-pure water with 2 % (v/v) of Triton X. After incubation for 1 h in a 37 ºC shaking water bath, samples were frozen at - 80 ºC. Samples were defrosted and used according to the manufacturer's recommendation (Quant-iT^{TM} PicoGreen® dsDNA assay kit, Life Technologies). A standard curve was obtained with the provided dsDNA solution. Samples were incubated during 10 min at RT. Fluorescence was read at an excitation wavelength of 485/20 nm and 528/20 nm of emission, using a microplate reader (Gen 5, Synergy HT, Biotek).

Metabolic activity: Mitochondrial metabolic activity quantification was performed using an MTS colorimetric assay (CellTiter96®, AQueous One Solution Cell, Promega) according to the manufacturer's recommendation. Briefly, at day 1, 4 and 7 of culture, macrophages (in triplicate) or liquefied capsules encapsulating ASCs (n=5 per well in triplicate) were incubated protected from light with the reagent kit (1:6 in PBS) for 4 h at 37 ºC in a humidified 5 % CO_2 air atmosphere. Then, absorbance was read at a wavelength of 490 nm using a microplate reader (Gen 5, Synergy HT, Biotek). MTS results were normalized with dsDNA quantification data.

Cytokine detection profiling: The amount of IL-6 and IL-10 (ELISA MAX™ Standard Set Human, Biolegend), as well as the concentration of human vascular endothelial growth factor (VEGF, Abcam) in the supernatants was assessed by ELISA quantification assay. For that, supernatants (500 µL) of cell culture media of macrophages and liquefied capsules (n=5 per well) were stored at -80ºC until analysis. Protein detection was performed according to each manufacture's specifications. Ultimately, the measurements were read at 450 nm in a microplate reader (Gen 5, Synergy HT, Biotek), and normalized with dsDNA quantification data.

Flow cytometry analysis: For the analysis of the surface markers, macrophages were detached from the well-plate by incubation with TrypLE^{TM} Express solution (Life Technologies) at 37 ºC for 5 min. Then, cells were incubated with Alexa Fluor® 647 anti-human CD163 antibody

(5 µL of antibody per $1x10^6$ of cells, clone RM3/1, Biolegend), Alexa Fluor® 488 anti-human CD80 antibody (5 µL of antibody per $1x10^6$ of cells, clone 2D10, Biolegend), and PE anti-human CD36 antibody for 45 min at 4 ºC and in the dark. Samples were acquired on a BD Accuri™ C6 Plus flow cytometer (BD Biosciences). All data were analysed using FlowJo™ Software (version 10, Ashland).

RNA Extraction and cDNA Production: The isolation of total RNA was performed using a column-based kit (PureLink™ RNA Mini Kit, ThermoFisher Scientific) according to manufacturer's specifications. Briefly, after 1, 4, and 7 days of culture, macrophages (in triplicate) were lysed with a Lysis Buffer containing 1 % of 2-mercaptoethanol and homogenized with a 21-gauge syringe. One volume of 70 % (v/v) of ethanol was added to each volume of cell homogenate, and then, the mix was entirely transferred to a spin cartridge. After several washes, the membrane-bounded RNA was eluted in RNase-free water and collected in single tubes. RNA quantity and purity were determined in a nanodrop spectrophotometer (NanoDrop ND-1000, ThermoFisher Scientific). Samples with a 260/280 purity ratio higher than ~2.0 were used for cDNA synthesis. The cDNA synthesis was performed using a SuperScript™ IV VILO™ Master Mix kit (ThermoFisher Scientific) and the ProFlex™ 2 x 96-well PCR System (ThermoFisher Scientific). All samples were normalized (1 ng of RNA per µL of RNase-free water).

Quantitative real-time polymerase chain reaction (qRT-PCR): The expression of inflammatory M1-like genes chemokine (C-X-C motif) ligand-10 (CXCL10), chemokine (C-C motif) ligand-20 (CCL20), as well as the expression of remodeling M2-like genes CD163 (cluster of differentiation 163), and CCL13, were quantified in the cDNA samples using a qRT-PCR reaction. The qRT-PCR was performed on a QuantStudio™ 3 Real-Time PCR system with the TaqMan® Fast Advanced Master Mix (ThermoFisher Scientific) and using TaqMan® gene expression assays (ThermoFisher Scientific), namely Hs00171138_m1 (CXCL11),

Hs01011368_m1 (CCL20), Hs00174705_m1 (CD163), and Hs00234646_m1 (CCL13). GAPDH (Hs99999905_m1, ThermoFisher Scientific) was used as the endogenous housekeeping control. Amplification profiles were analyzed with QuantStudio™ Design and Analysis Software v1.5.1 (ThermoFisher Scientific). The relative expression levels of each gene in cells were normalized to the GAPDH gene using the $2^{-\Delta\Delta Ct}$ method (Perkin-Elmer). Three independent experiments were performed.

Statistical analysis: Statistical analysis was performed using one- and two-way analysis of variance (ANOVA) with Tukey's post-hoc test (GraphPad Prism 6.0). p-values <0.05 were considered statistically significant. All results are presented as mean ± standard deviation.

Acknowledgements

The authors acknowledge the financial support given by the Portuguese Foundation for Science and Technology (FCT) with the doctoral grant of Sara Nadine (SFRH/BD/130194/2017), the project "CIRCUS" (PTDC/BTM-MAT/31064/2017), and the European Research Council for the project "ATLAS" (ERC-2014-AdG-669858). This work was developed within the scope of the project CICECO-Aveiro Institute of Materials, UIDB/50011/2020 & UIDP/50011/2020, financed by national funds through the FCT/MEC and when appropriate co-financed by FEDER under the PT2020 Partnership Agreement.

Received: ((will be filled in by the editorial staff))
Revised: ((will be filled in by the editorial staff))
Published online: ((will be filled in by the editorial staff))

References

[1] D. F. Williams, *Biomaterials* **2008**, *29*, 2941.

[2] Z. Julier, A. J. Park, P. S. Briquez, M. M. Martino, *Acta Biomater.* **2017**, *53*, 13.

[3] T. A. Wynn, K. M. Vannella, *Immunity* **2016**, *44*, 450.

[4] A. Vishwakarma, N. S. Bhise, M. B. Evangelista, J. Rouwkema, M. R. Dokmeci, A. M. Ghaemmaghami, N. E. Vrana, A. Khademhosseini, *Trends Biotechnol.* **2016**, *34*, 470.

[5] S. Franz, S. Rammelt, D. Scharnweber, J. C. Simon, *Biomaterials* **2011**, *32*, 6692.

[6] E. Mariani, G. Lisignoli, R. M. Borzì, L. Pulsatelli, *Int. J. Mol. Sci.* **2019**, *20*, 42.

[7] V. Gribova, R. Auzely-Velty, C. Picart, J. Fourier, **2011**.

[8] I. M. Bjørge, I. S. Choi, C. R. Correia, J. F. Mano, *Nanoscale* **2019**, *11*, 16214.

[9] H. Y. Huh, S. F. Pearce, L. M. Yesner, J. L. Schindler, R. L. Silverstein, *Blood* **1996**, *87*, 2020.

[10] T. Taniguchi, Y. Koido, J. Aiboshi, T. Yamashita, S. Suzaki, A. Kurokawa, *Crit. Care Med.* **1999**, *27*, 1262.

[11] S. Ruiz, F. Vardon-Bounes, V. Merlet-Dupuy, J.-M. Conil, M. Buléon, O. Fourcade, I. Tack, V. Minville, *Intensive Care Med. Exp.* **2016**, *4*, 22.

[12] C. R. Correia, R. P. Pirraco, M. T. Cerqueira, A. P. Marques, R. L. Reis, J. F. Mano, *Sci. Rep.* **2016**, *6*, 21883.

[13] S. A. Eming, T. Krieg, *J. Investig. dermatology. Symp. Proc.* **2006**, *11*, 79.

[14] B. N. Brown, S. F. Badylak, *Acta Biomater.* **2013**, *9*, 4948.

[15] J. M. Anderson, A. Rodriguez, D. T. Chang, *Semin. Immunol.* **2008**, *20*, 86.

[16] B. N. Brown, B. D. Ratner, S. B. Goodman, S. Amar, S. F. Badylak, *Biomaterials* **2012**, *33*, 3792.

[17] S. Gordon, P. R. Taylor, *Nat. Rev. Immunol.* **2005**, *5*, 953.

[18] C. D. Mills, K. Kincaid, J. M. Alt, M. J. Heilman, A. M. Hill, *J. Immunol.* **2000**, *164*, 6166 LP.

[19] D. M. Mosser, J. P. Edwards, *Nat. Rev. Immunol.* **2008**, *8*, 958.

[20] C. R. Correia, J. Gaifem, M. B. Oliveira, R. Silvestre, J. F. Mano, *Biomater. Sci.* **2017**, *5*, 551.

[21] M. B. Oliveira, J. F. Mano, *Trends Biotechnol.* **2014**, *32*, 627.

[22] C. R. Correia, S. Gil, R. L. Reis, J. F. Mano, *Adv. Healthc. Mater.* **2016**, *5*, 1346.

[23] C. R. Correia, R. L. Reis, J. F. Mano, *Biomacromolecules* **2013**, *14*, 743.

[24] C. R. Correia, T. C. Santos, R. P. Pirraco, M. T. Cerqueira, A. P. Marques, R. L. Reis, J. F. Mano, *Acta Biomater.* **2017**, *53*, 483.

[25] S. Nadine, S. G. Patrício, C. R. Correia, J. F. Mano, *Biofabrication* **2019**, *12*, 15005.

[26] S. Nadine, S. G. Patrício, C. C. Barrias, I. S. Choi, M. Matsusaki, C. R. Correia, J. F. Mano, *Adv. Biosyst.* **2020**, *n/a*, 2000127.

[27] J. Borges, J. F. Mano, *Chem. Rev.* **2014**, *114*, 8883.

[28] F. Y. McWhorter, T. Wang, P. Nguyen, T. Chung, W. F. Liu, *Proc. Natl. Acad. Sci.* **2013**, *110*, 17253 LP.

[29] A. R. D. Reeves, K. L. Spiller, D. O. Freytes, G. Vunjak-Novakovic, D. L. Kaplan, *Biomaterials* **2015**, *73*, 272.

[30] K. L. Spiller, S. Nassiri, C. E. Witherel, R. R. Anfang, J. Ng, K. R. Nakazawa, T. Yu, G. Vunjak-Novakovic, *Biomaterials* **2015**, *37*, 194.

[31] G. E. Glass, J. K. Chan, A. Freidin, M. Feldmann, N. J. Horwood, J. Nanchahal, *Proc. Natl. Acad. Sci.* **2011**, *108*, 1585 LP.

[32] K. Schmidt-Bleek, H. Schell, N. Schulz, P. Hoff, C. Perka, F. Buttgereit, H.-D. Volk, J. Lienau, G. N. Duda, *Cell Tissue Res.* **2012**, *347*, 567.

[33] K. N. Couper, D. G. Blount, E. M. Riley, *J. Immunol.* **2008**, *180*, 5771 LP.

[34] A. King, S. Balaji, L. D. Le, T. M. Crombleholme, S. G. Keswani, *Adv. wound care* **2014**, *3*, 315.

[35] W. C. W. Chen, B. G. Lee, D. W. Park, K. Kim, H. Chu, K. Kim, J. Huard, Y. Wang, *Biomaterials* **2015**, *72*, 138.

[36] D. R. Cole, M. Waterfall, M. McIntyre, J. D. Baird, *Diabetologia* **1992**, *35*, 231.

[37] G. Orive, S. Ponce, R. M. Hernández, A. R. Gascón, M. Igartua, J. L. Pedraz, *Biomaterials* **2002**, *23*, 3825.

[38] T. Espevik, M. Otterlei, G. Skjåk-Braek, L. Ryan, S. D. Wright, A. Sundan, *Eur. J. Immunol.* **1993**, *23*, 255.

[39] A. Boddupalli, L. Zhu, K. M. Bratlie, *Adv. Healthc. Mater.* **2016**, *5*, 2575.

[40] O. Veiseh, J. C. Doloff, M. Ma, A. J. Vegas, H. H. Tam, A. R. Bader, J. Li, E. Langan,

J. Wyckoff, W. S. Loo, S. Jhunjhunwala, A. Chiu, S. Siebert, K. Tang, J. Hollister-Lock, S. Aresta-Dasilva, M. Bochenek, J. Mendoza-Elias, Y. Wang, M. Qi, D. M. Lavin, M. Chen, N. Dholakia, R. Thakrar, I. Lacík, G. C. Weir, J. Oberholzer, D. L. Greiner, R. Langer, D. G. Anderson, *Nat. Mater.* **2015**, *14*, 643.

[41] A. Mantovani, A. Sica, S. Sozzani, P. Allavena, A. Vecchi, M. Locati, *Trends Immunol.* **2004**, *25*, 677.

[42] R. A. Quirk, W. C. Chan, M. C. Davies, S. J. B. Tendler, K. M. Shakesheff, *Biomaterials* **2001**, *22*, 865.

[43] B. L. Strand, T. L. Ryan, P. In't Veld, B. Kulseng, A. M. Rokstad, G. Skjak-Brek, T. Espevik, *Cell Transplant.* **2001**, *10*, 263.

[44] S. Juste, M. Lessard, N. Henley, M. Menard, J.-P. Halle, *J. Biomed. Mater. Res. A* **2005**, *72*, 389.

[45] Y. Duan, H. Zheng, Z. Li, Y. Yao, J. Ding, X. Wang, J. R. Nakkala, D. Zhang, Z. Wang, X. Zuo, X. Zheng, J. Ling, C. Gao, *Biomaterials* **2020**, 120012.

[46] E. I. Rabea, M. E.-T. Badawy, C. V Stevens, G. Smagghe, W. Steurbaut, *Biomacromolecules* **2003**, *4*, 1457.

[47] D. P. Vasconcelos, C. de Torre-Minguela, A. I. Gomez, A. P. Aguas, M. A. Barbosa, P. Pelegrin, J. N. Barbosa, *Acta Biomater.* **2019**, *91*, 123.

[48] D. Fong, P. Gregoire-Gelinas, A. P. Cheng, T. Mezheritsky, M. Lavertu, S. Sato, C. D. Hoemann, *Biomaterials* **2017**, *129*, 127.

[49] M. I. Oliveira, S. G. Santos, M. J. Oliveira, A. L. Torres, M. A. Barbosa, *Eur. Cell. Mater.* **2012**, *24*, 133.

[50] S. Gudmundsdottir, R. Lieder, O. E. Sigurjonsson, P. H. Petersen, *J. Biomed. Mater. Res. A* **2015**, *103*, 2778.

[51] D. P. Vasconcelos, A. C. Fonseca, M. Costa, I. F. Amaral, M. A. Barbosa, A. P. Aguas, J. N. Barbosa, *Biomaterials* **2013**, *34*, 9952.

[52] R. Dai, Z. Wang, R. Samanipour, K. Koo, K. Kim, *Stem Cells Int.* **2016**, *2016*, 6737345.

[53] K. L. Spiller, R. R. Anfang, K. J. Spiller, J. Ng, K. R. Nakazawa, J. W. Daulton, G. Vunjak-Novakovic, *Biomaterials* **2014**, *35*, 4477.

[54] C. Stockmann, S. Kirmse, I. Helfrich, A. Weidemann, N. Takeda, A. Doedens, R. S. Johnson, *J. Invest. Dermatol.* **2011**, *131*, 797.

[55] F. Verseijden, H. Jahr, S. J. Posthumus-van Sluijs, T. L. Ten Hagen, S. E. R. Hovius, A. L. B. Seynhaeve, J. W. van Neck, G. J. V. M. van Osch, S. O. P. Hofer, *Tissue Eng. Part A* **2008**, *15*, 445.

[56] J. H. Kang, J. M. Gimble, D. L. Kaplan, *Tissue Eng. Part A* **2009**, *15*, 2227.

[57] L. Chen, E. E. Tredget, P. Y. G. Wu, Y. Wu, Y. Wu, *PLoS One* **2008**, *3*, 1886.

[58] S. E. Hanson, S. N. King, J. Kim, X. Chen, S. L. Thibeault, P. Hematti, *Tissue Eng. Part A* **2011**, *17*, 2463.

[59] D. A. Cantu, P. Hematti, W. J. Kao, *Stem Cells Transl. Med.* **2012**, *1*, 740.

[60] M. D. Swartzlander, A. K. Blakney, L. D. Amer, K. D. Hankenson, T. R. Kyriakides, S. J. Bryant, *Biomaterials* **2015**, *41*, 79.

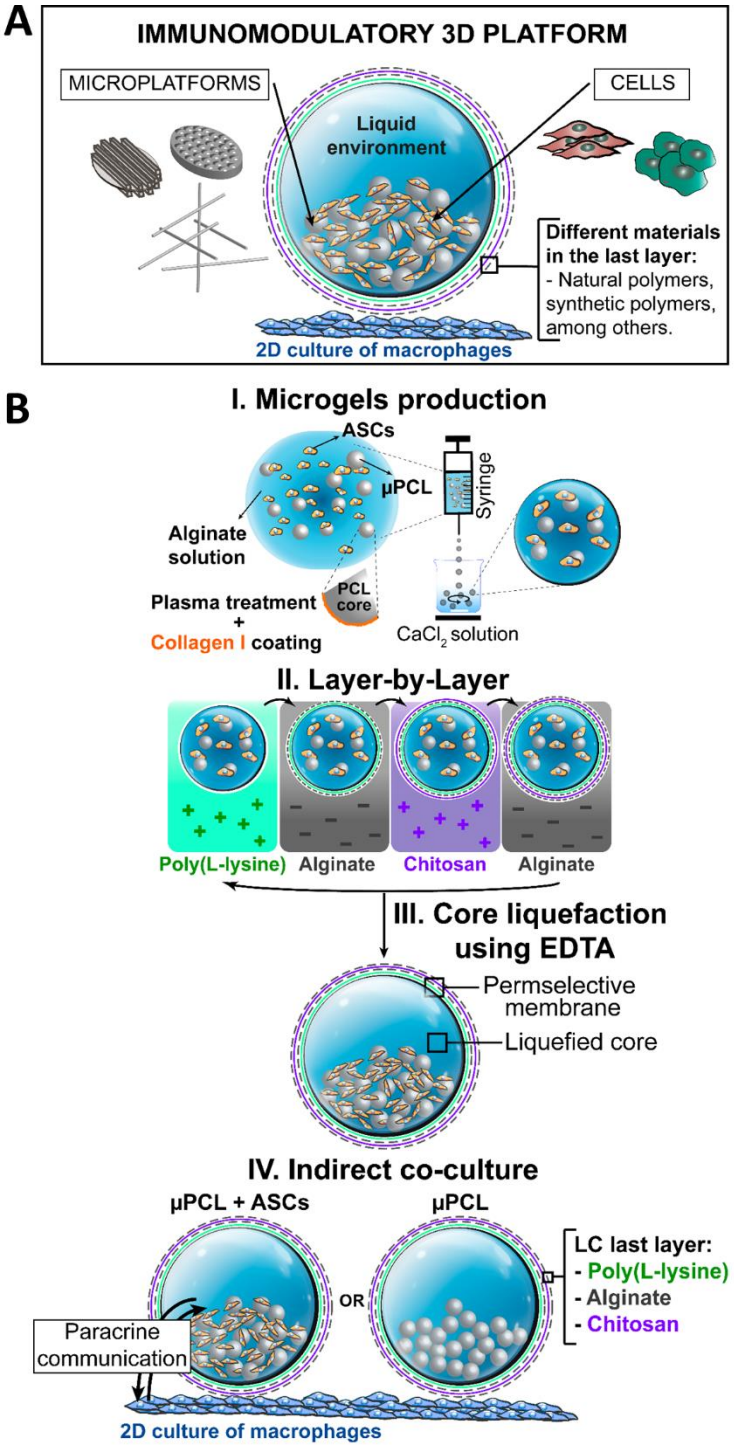

Scheme 1. A. Immunomodulatory miniaturized 3D platform using liquefied capsules for the *in vitro* high-throughput combinatorial screening of different biomaterials, cells, and bioinstructive microplatforms. **B.** Production and culture of the liquefied capsules: I. Microgels are obtained by the ionotropic gelation of alginate containing adipose-derived mesenchymal stem cells (ASCs) and surface functionalized poly(ε-caprolactone) microparticles (μPCL) in calcium chloride (CaCl2) solution. II. Then, in order to produce a permselective nano-layered membrane, the layer-by-layer technique is performed using three different polyelectrolytes, namely poly(L-lysine) (PLL), alginate (ALG), and chitosan (CHT). III. The liquefied core is obtained by chelation with ethylenediaminetetraacetic acid (EDTA). IV. Three different encapsulation systems are developed, each one ending with a different

polyelectrolyte, namely PLL, ALG, or CHT. Ultimately, the different immunomodulatory 3D platform with or without cells are added on top of 2D culture of macrophages.

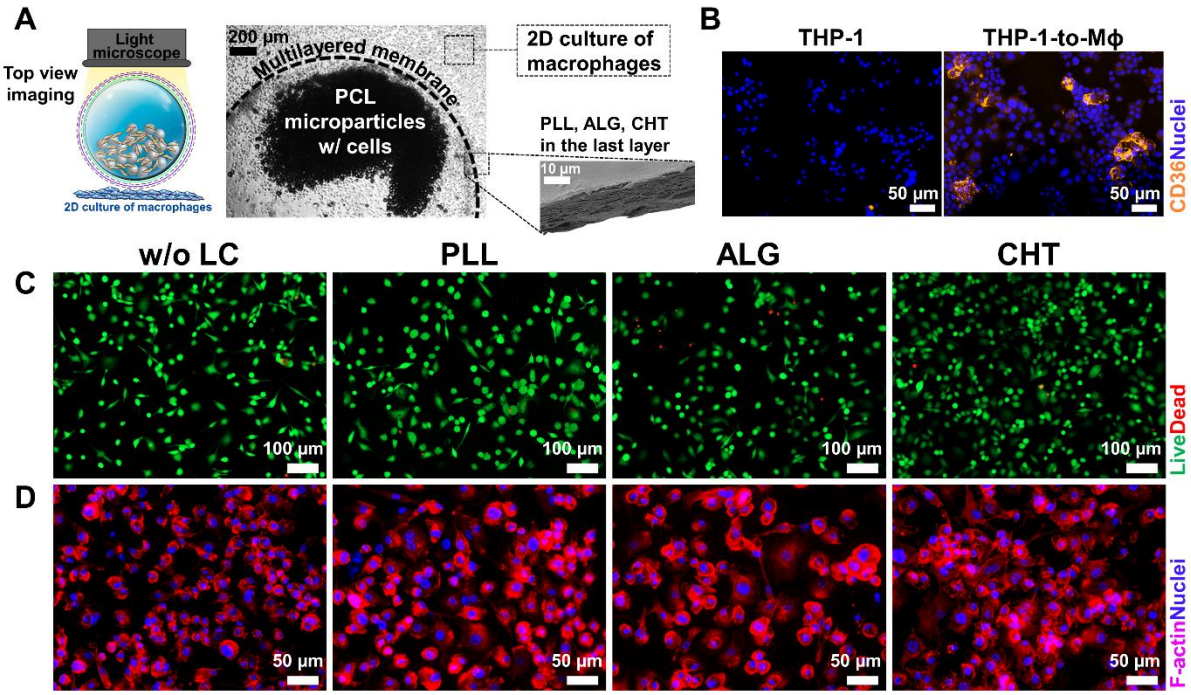

Figure 1. A. Top view light microscopy of Liquefied Capsules (LC) encapsulating poly(ε-caprolactone) microparticles (µPCL) on top of a 2D culture of THP-1 macrophages. The stratification of the nanolayered membrane is observed by scanning electron microscopy. **B.** THP-1 monocyte differentiation into macrophages (Mϕ). THP-1 cells were incubated for 24 h in the presence of 50 nM of phorbol myristate acetate (PMA), and additional 24 h in RPMI medium. Cells were then fixed and immunolabeled for CD36-PE (orange). Nuclei were counterstained with DAPI (blue). **C.** Live-dead fluorescence assay of macrophages cultured with LC ending in poly(L-lysine) (PLL), alginate (ALG), or chitosan (CHT), after 7 days of culture. Macrophages without interaction with LC were used as control (w/o LC). Living cells were stained by calcein (green) and dead cells by propidium iodide (red). **D.** DAPI-phalloidin fluorescence assay of macrophages cultured with LC ending in PLL, ALG or CHT, after 7 days of culture. Macrophages without interaction with LC were used as control (w/o LC). Cells nuclei were stained by DAPI (blue) and F-actin filaments by phalloidin (pink).

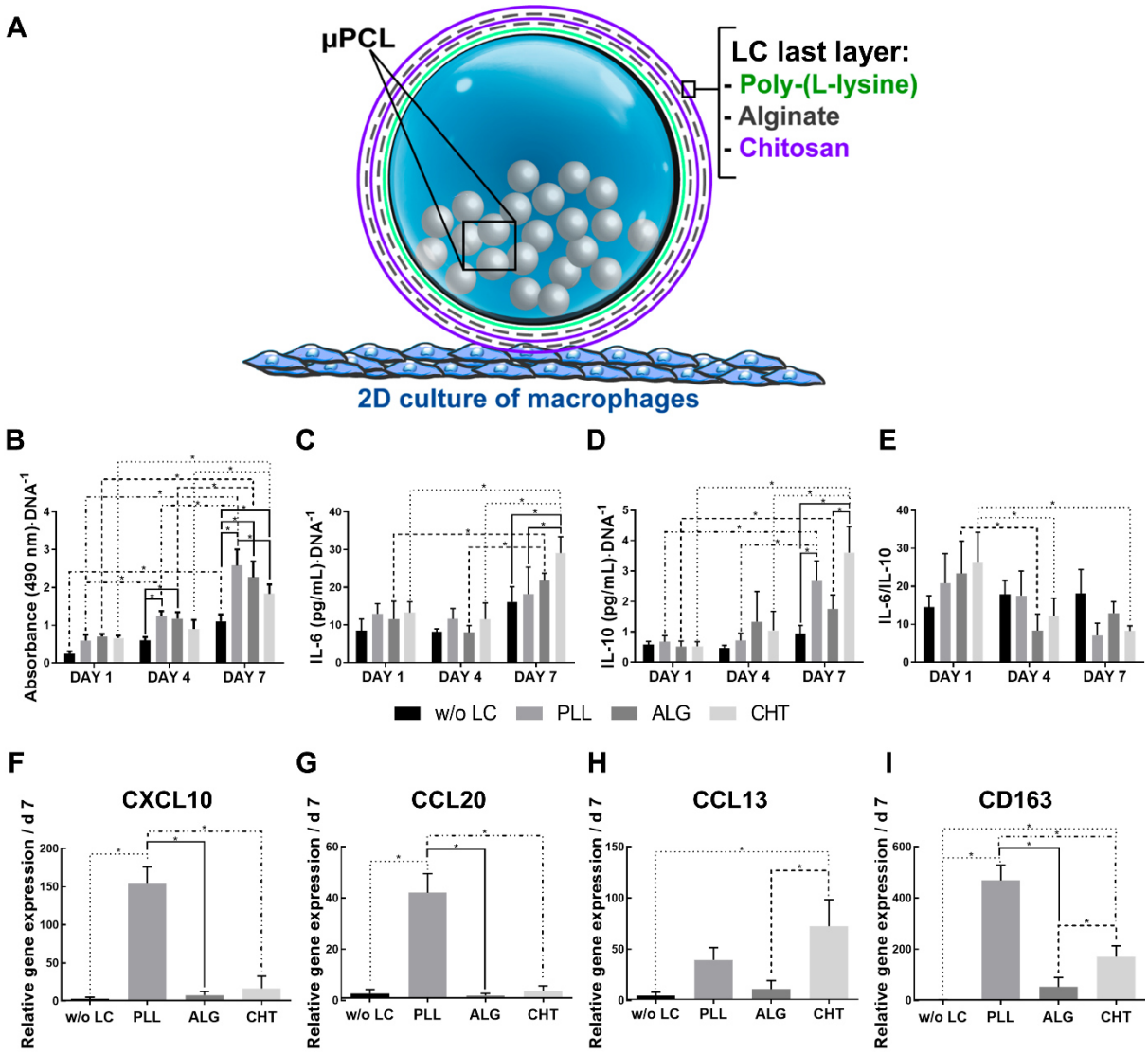

Figure 2. A. Influence of Liquefied Capsules (LC) encapsulating poly(ε-caprolactone) microparticles (μPCL) and ending in poly(L-lysine) (PLL), alginate (ALG), or chitosan (CHT), in the polarization of macrophages. **B.** Cell metabolic activity determined by MTS colorimetric assay of macrophages after 1, 4, and 7 days of culture. Results were normalized with DNA content. **C-E.** IL-6, IL-10, and IL-6/IL-10 ratio quantification by ELISA of macrophages after 1, 4, and 7 days of culture. Results were normalized with DNA content. Gene expression of (**F-G**) pro-inflammatory CXCL10 and CCL20, and (**H-I**) anti-inflammatory CCL13 and CD163 markers at 7 days of 2D macrophages culture. *p*-values < 0.05 were considered statistically significant (*$p < 0.05$).

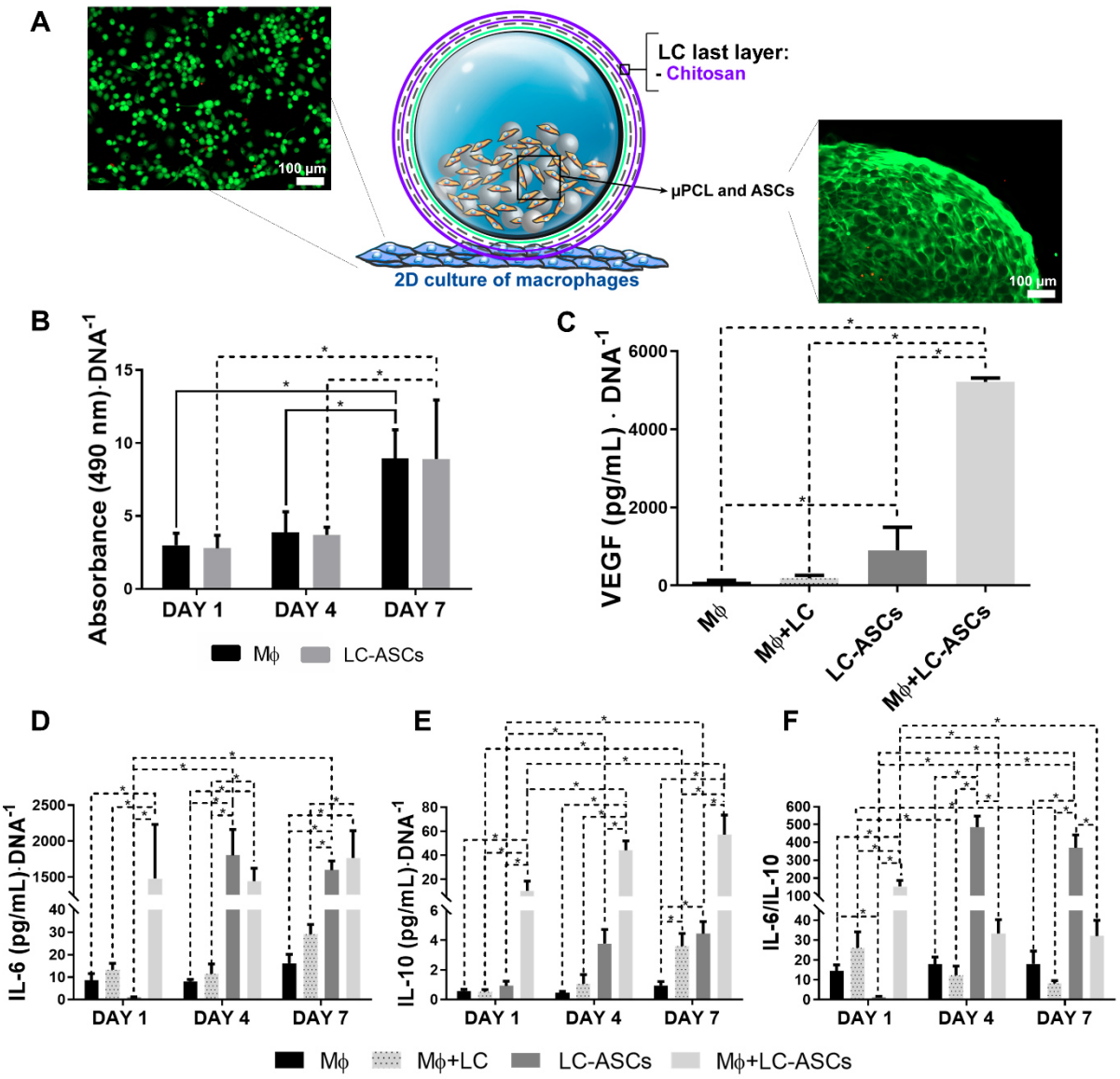

Figure 3. A. Indirect co-culture between encapsulated adipose-derived mesenchymal stem cells (LC-ASCs) on chitosan-ending liquefied capsules cultured on top of a 2D culture of macrophages (Mϕ). Live-dead fluorescence assay in macrophages (left) and encapsulated ASCs and poly(ε-caprolactone) microparticles (µPCL) (right), after 7 days of culture. Living cells were stained by calcein (green) and dead cells by propidium iodide (red). **B.** Cell metabolic activity determined by MTS colorimetric assay of macrophages and encapsulated ASCs after 1, 4, and 7 days of culture. Results were normalized with DNA content. **C.** Quantification of released VEGF by ELISA after 7 days of culture. Results were normalized with DNA content. **D-F.** IL-6, IL-10, and IL-6/IL-10 ratio quantification by ELISA of macrophages and ASCs after 1, 4, and 7 days of culture. Results were normalized with DNA content. *p*-values < 0.05 were considered statistically significant (*$p < 0.05$).

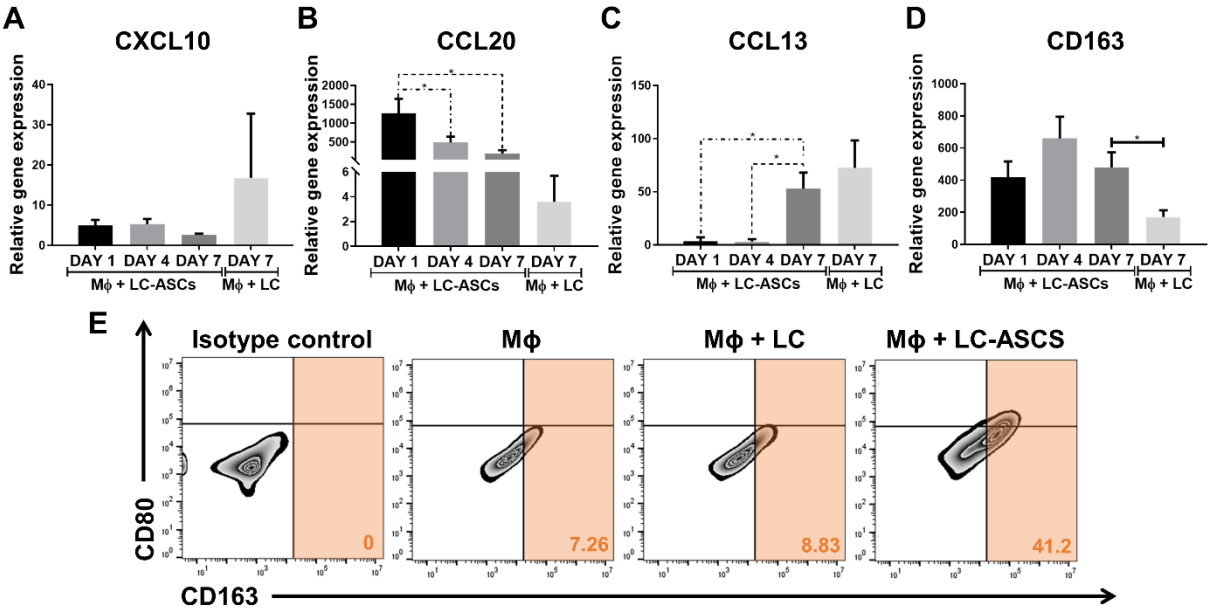

Figure 4. Impact of encapsulated adipose-derived mesenchymal stem cells (ASCs) over macrophage polarization after 1, 4, and 7 days of culture, and respective comparation without encapsulated ASCs at day 7 of culture. **A-B.** Relative expression of pro-inflammatory CXCL10 and CCL20 markers of macrophages. **C-D.** Relative expression of anti-inflammatory CCL13 and CD163 markers of macrophages. **E.** Cell surface expression of CD80 and CD163 in macrophages cultured for 7 days of culture alone (Mϕ), or in contact with cell-empty liquefied capsules ending in chitosan (Mϕ+LC) or encapsulating adipose-derived mesenchymal stem cells (Mϕ+LC-ASCs). Orange shadow represents the percentage of CD163 marker expression. *p*-values < 0.05 were considered statistically significant (*p < 0.05).

S. Nadine, C. R. Correia*, J. F. Mano*

An immunomodulatory miniaturized screening 3D platform using liquefied capsules

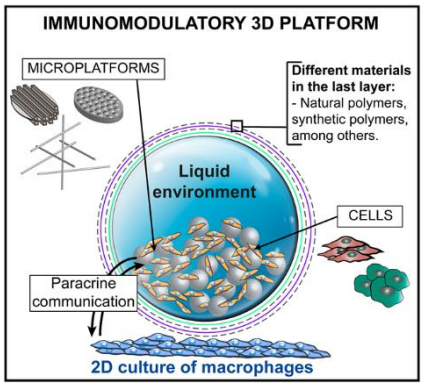

Immunomodulatory miniaturized 3D platform using liquefied capsules for the *in vitro* high-content combinatorial screening of different biomaterials, cells, and bioinstructive microplatforms. Simply by changing the biomaterial of the last layer of the liquefied capsules, it is possible to proactively modulate the surrounding macrophages behavior, and at the same time, study independently the paracrine signaling with encapsulated cells.

Supporting Information

An immunomodulatory miniaturized screening 3D platform using liquefied capsules

Sara Nadine, Clara R. Correia, João F. Mano**

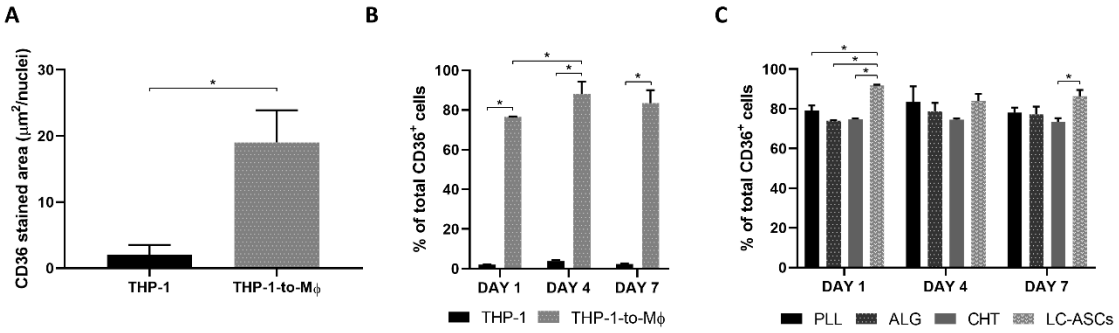

Figure S1. Expression of the macrophage marker CD36. **A.** Semi-quantitative analysis of CD36 in THP-1 monocytes and THP-1 differentiated macrophages (THP-1-to-Mϕ). CD36 stained area was calculated from thresholded images using ImageJ software. **B.** Cell surface expression of CD36 in monocytes and macrophages after 7 days of culture. **C.** Cell surface expression of CD36 in macrophages cultured for 7 days in contact with cell-empty liquefied capsules ending in poly(L-lysine) (PLL), alginate (ALG), and chitosan (CHT) or encapsulating adipose-derived mesenchymal stem cells (LC-ASCs). *p*-values < 0.05 were considered statistically significant (**p* < 0.05).

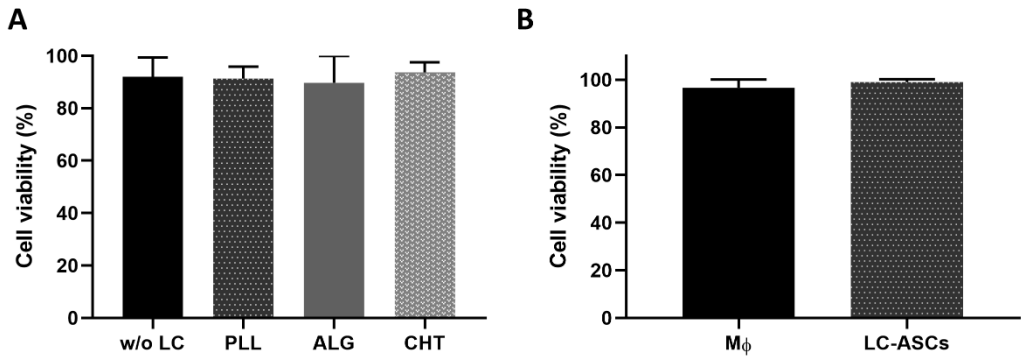

Figure S2. A. Live-dead assay of macrophages cultured with empty liquefied capsules (LC) ending in poly(L-lysine) (PLL), alginate (ALG), or chitosan (CHT), after 7 days of culture. Macrophages without interaction with LC were used as control (w/o LC). ImageJ software was used to perform the cell viability quantification. **B.** Live-dead quantification assay of macrophages and encapsulated adipose-derived mesenchymal stem cells (ASCs), after 7 days of indirect co-culture. Encapsulated ASCs (LC-ASCs) on chitosan-ending liquefied capsules were cultured on top of a 2D culture of macrophages (Mϕ). ImageJ software was used to perform the cell viability quantification. *p*-values < 0.05 were considered statistically significant (***p** < 0.05).

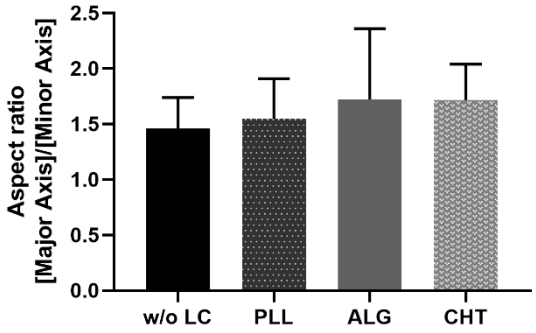

Figure S3. The aspect ratio of macrophages was analyzed after 7 days of culture with empty liquefied capsules (LC) ending in poly(L-lysine) (PLL), alginate (ALG), or chitosan (CHT). The elongation of the cells, defined by the [Major Axis]/[Minor Axis] ratio, was quantified using DAPI-Phalloidin images by the ImageJ software. *p*-values < 0.05 were considered statistically significant (**p* < 0.05).

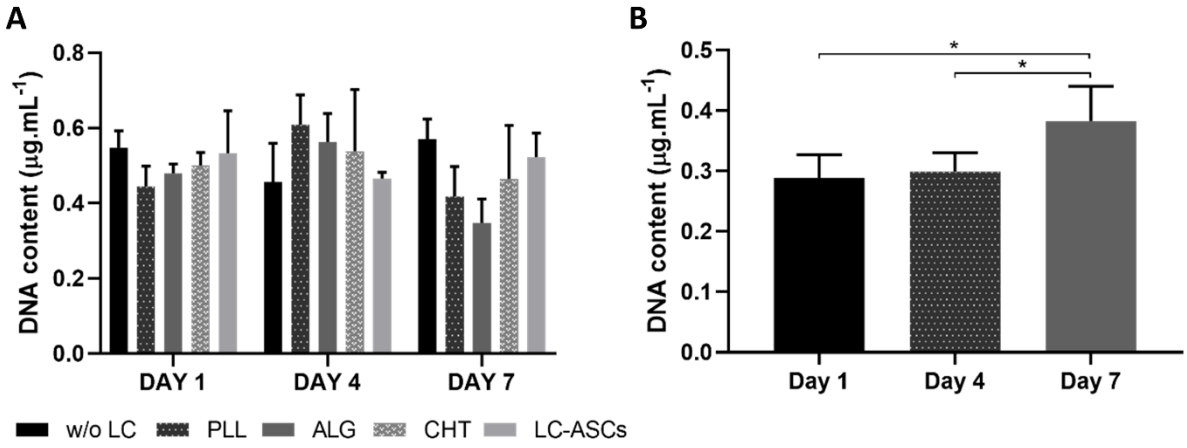

Figure S4. Cell proliferation assay by DNA quantification of: **A.** Macrophages cultured with empty liquefied capsules (LC) ending in poly(L-lysine) (PLL), alginate (ALG), chitosan (CHT), or cultured with encapsulated adipose-derived mesenchymal stem cells (LC-ASCs) on chitosan-ending liquefied capsules, after 7 days of culture. Macrophages without interaction with LC were used as control (w/o LC). **B.** Adipose-derived mesenchymal stem cells (ASCs) encapsulated on chitosan-ending liquefied capsules, after 7 days of culture. *p*-values < 0.05 are considered statistically significant (*$p < 0.05$).